Existence and Reactivity of Three Forms of Orthophthalaldehyde in Aqueous Solutions. Polarographic, Voltammetric, and Spectrophotometric Study

Nuha Salem, Silvana Andreescu, Eliona Kulla, and Petr Zuman*

Department of Chemistry, Clarkson University, Potsdam, New York 13699-5810

Received: February 10, 2007; In Final Form: March 29, 2007

Orthophthalaldehyde (1,2-dicarboxaldehyde) (OPA) forms in the presence of a strong nucleophile with amino acids isoindole derivatives. The reaction is used in fluorometric determination of amino acids. The mechanism of these processes is not understood. OPA is present in aqueous solutions in three forms: unhydrated (I_a), monohydrated acyclic (I_b), and cyclic hemiacetal (I_c). The absence of data for the molar absorptivities of these forms, together with overlap of their absorption bands, limits the application of spectrophotometry. Measurement of polarographic limiting currents of forms I_a and I_b enables determination of equilibrium constants K_1 (formation of I_b) and K_2 (for the ring formation). The presence of these forms was supported by ^{1}H NMR and ^{13}C NMR. The rate of hydration of OPA is general-acid−base-catalyzed, but that of dehydration shows only specific-acid−base catalysis. The rate of hydration is controlled by general-acid−base-catalyzed addition of water to I_a. The rate of dehydration depends on the opening of the ring in I_c, which is specific-acid−base-catalyzed. At pH > 10 OPA undergoes a complex set of acid−base reactions (Scheme 3). The presence of polarographic anodic waves and oxidation on the gold electrode indicates the importance of the presence of a geminal diol form (II_a). Establishment of equilibria among the three forms of OPA together with reactions at pH > 10 has to be considered in elucidating the reaction scheme of procedures using OPA as a reagent in the determination of amino acids.

Introduction

Solutions of orthophthalaldehyde (benzene-1,2-dicarboxaldehyde) (OPA) are frequently used in the determination of amino acids. In a typical procedure[1] a nucleophile—most frequently thiolate or cyanide ion—is added to a solution of OPA in a buffer at pH 8−11. To the resulting reagent is added a sample of amino acid, and a fluorophore is formed. It was proved[2] that the fluorescent species is an isoindole derivative. Typically, these fluorescent species may undergo consecutive reactions resulting in a decrease of the measured fluorescence. The mechanism by which the isoindole derivative is formed is not understood.[3] On the basis of product identification, some possible reaction schemes were presented.[2f,3b,4] Among limitations of these schemes, discussed elsewhere,[1h] is the absence of an understanding of the solution chemistry of OPA, the nature of the reaction with the added nucleophile present in excess, and an assumption of a rapid cleavage of a C−H bond. The proposed mechanism involved a sequence of equilibria, but no attempts have been made to investigate any of them separately. Hence, no information is available about the values of the equilibrium constants involved. The limited investigations of the kinetics[1d,f,3b] were carried out in a ternary reaction mixture, containing OPA, the strong nucleophile present in excess, and the reacting amino acid. Interpretation of the kinetics in such a reaction mixture is too complex. No additional mechanistic information has been obtained for the analogous reaction of 2,3-naphthalenedicarboxaldehyde, which was more recently proposed to replace OPA[5] due to the higher stability of the isoindole derivative.

For a better understanding of the processes involved in the determination of amino acids, it was first necessary to obtain information about the equilibria of the species present in solutions of OPA and about the kinetics of their establishment.

Little attention has been paid in the past to the solution chemistry of OPA. It has been generally assumed that OPA is in aqueous solutions "extensively hydrated and the hydrate exists extensively as the cyclic 1,3-phthalandiol" (I_c).[6] An early report[7] on the formation of a monohydrate, based on measurement of the melting point of an OPA−water mixture, was considered[6] erroneous. In some instances the presence of the unhydrated form (I_a) was considered, but no attempt has been reported to determine its equilibrium concentration, even when this form seems particularly prone to a nucleophilic attack.

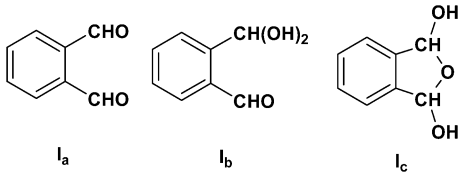

I_a I_b I_c

In three papers[8] which remained unnoticed, a polarographic reduction of OPA in two steps has been reported. The first step at the most positive potentials was attributed to a reduction of the unhydrated form (I_a) and the second to the reduction of the formyl group of the acyclic monohydrated form (I_b). The cyclic hemiacetal form (I_c) is not reducible in the available potential range, but its concentration can be obtained from known concentrations of I_a and I_b and the known initial concentration of OPA. In these papers[8] no effort has been made to evaluate the equilibrium concentrations of forms I_a, I_b, and I_c. Attempts to determine the number of electrons in each reduction step[8c]

* To whom correspondence should be addressed. E-mail: zumanp@clarkson.edu. Phone: (315) 268-2340. Fax: (315) 268-6610.

10.1021/jp071151s CCC: $37.00
Published on Web 05/09/2007

were complicated by bulk chemical reactions in the course of preparative electrolysis.

In this study, polarography using a dropping mercury electrode, voltammetry carried out with glassy carbon and gold electrodes, and recording UV and NMR spectra were used in the investigation of the solution chemistry of OPA. Both reduction waves of the unhydrated formyl groups and oxidation waves involving geminal diol anions formed at pH > 10 were followed. Hydration−dehydration equilibria as well as equilibria corresponding to addition of hydroxide ions to OPA were investigated, as well as the rates of hydration and dehydration and ring formation and opening.

Experimental Section

Instruments. The polarographic current−voltage curves were recorded using a Sargent polarograph, model XVI (E. H. Sargent and Co.). The dropping mercury electrode (DME) used had the following characteristics: $m = 2.2$ mg s^{-1}, $t_1 = 5.0$ s, and at $h = 64$ cm. A Kalousek cell,[9] with a reference electrode separated by a liquid junction, was used for dc polarography. A jacketed cell with water circulated from a thermostat and a separated reference electrode was used for the variable-temperature experiments. The reference electrode was a saturated calomel electrode (SCE). The temperature in the electrochemical cells was controlled using a PolyScience heating circulator, model 80.

Cyclic voltammetry (CV) experiments were performed using an Epsilon potentiostat (Bioanalytical System Inc., West Lafayette, IN). The cell for the CV experiments was a conventional electrochemical cell equipped with a Ag/AgCl/3 M NaCl (BAS MF-2052, RE-5B) reference electrode and a platinum wire (BAS MW-1032) as the counter electrode. A glassy carbon electrode (GCE) (BAS MF-2012 with a diameter of 3.0 mm) and a gold electrode (GE) (BAS MF-2072 with a diameter of 1.6 mm) were used as the working electrodes.

UV−vis absorption spectra were recorded using a Hewlett-Packard Agilent 8453 UV−vis spectrophotometer with a 10 mm quartz cell and a Shimadzu 2401PC UV−vis spectrophotometer equipped with a temperature control unit.

A Denver Instruments, model UB-10, pH meter equipped with a glass electrode was used for the pH measurements.

NMR experiments were carried out using a Bruker DMX 400 AVANCE NMR spectrometer equipped with a 5 mm BBO probe with a *z* gradient and a temperature control unit.

Materials. OPA was supplied by Ralph N. Emanuel Ltd. and used without further purification. Isophthalaldehyde (IPA) and terephthalaldehyde (TPA) were purchased from Aldrich. Acetonitrile was used to prepare stock solutions of orthophthalaldehyde and in some reaction mixtures was obtained from J. T. Baker. Chemicals used for buffer preparation (sodium acetate, boric acid, primary and secondary sodium phosphate, hydrochloric acid, sulfuric acid, phosphoric acid, and sodium hydroxide) were all of analytical grade. Potassium chloride used for controlling the ionic strength was obtained from Fisher Scientific. Deuterated solvents used for NMR measurements, D_2O and CD_3CN (99.8% D atom), were purchased from Acros and Cambridge Isotope Laboratories Inc., respectively. Acetone (HPLC grade, ≥99.9%) used to prepare the internal standard for the NMR measurements was obtained from Aldrich.

Solutions. Stock solutions of OPA and IPA (and TPA for UV spectra) were prepared in acetonitrile as follows: 0.01 M for polarography and spectrophotometric measurements and 0.3 M for CV measurements. Stock solutions of dialdehydes were kept in the dark, refrigerated, and used not more than two weeks after preparation. Samples of 14.0 mg of OPA and IPA were dissolved directly in 1.0 mL of CD_3CN or a CD_3CN/D_2O mixture for the NMR measurements. Buffer solutions of pH 1−3.2, 5.8−7.8, and 10.5−12.5 (phosphate buffers) were prepared using $H_3PO_4/NaH_2PO_4{\cdot}2H_2O$, $NaH_2PO_4{\cdot}2H_2O/Na_2HPO_4$, and $Na_2HPO_4/Na_3PO_4{\cdot}12H_2O$, respectively. Buffers of pH 3.7−5.7 (acetate buffers) were prepared using $CH_3COOH/CH_3COONa{\cdot}3H_2O$, and buffers of pH 8−10.3 were prepared using H_3BO_3/NaOH. The acid and base components of each buffer were mixed in a ratio needed to obtain the desired pH value, based on the Henderson−Hasselbach equation. All buffers were prepared fresh every two weeks. Water used to prepare the buffers and other aqueous solutions was deionized. Sodium hydroxide solutions were prepared using carbonate-free deionized water.

H_2O/CH_3CN solutions containing 50−97% H_2O were used for recording the UV spectra and CV using GCE. D_2O/CD_3CN solutions used in the NMR measurements were in the range 20−65% D_2O.

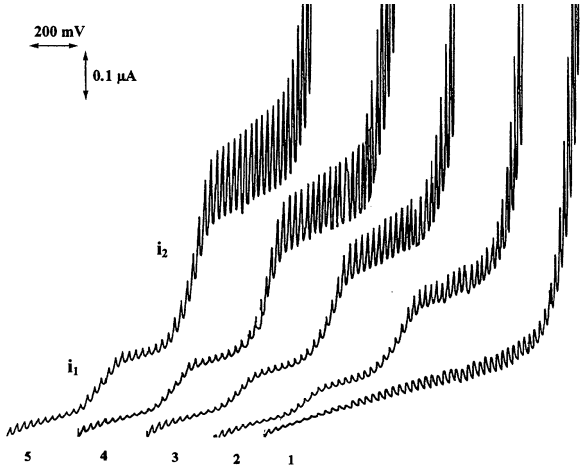

Figure 1. Dependence of polarographic $i-E$ waves of reduction of orthophthalaldehyde in a phosphate buffer, pH 5.8, on the concentration of the aldehyde: (1) 0.0 mM, (2) 0.04 mM, (3) 0.08 mM, (4) 0.12 mM, (5) 0.16 mM. Curves were recorded starting at −0.4 V.

Procedures. For polarography 100 μL of a 0.01 M stock solution of a dialdehyde in acetonitrile was added to 9.90 mL of buffer solution (phosphate, acetate, or borate), sodium hydroxide solution of the desired pH, or buffer solutions containing 29% acetonitrile. The pH meter was calibrated using standard buffers of the same acetonitrile contents as the solution under study. The final concentrations of acetonitrile were 1% and 30%, and the final concentration of dialdehydes was 1×10^{-4} M. For experiments where the buffer concentration was varied, a solution of potassium chloride was added to keep the ionic strength constant. Polarographic current−voltage curves were recorded after purging with N_2 for oxygen removal for about 2 min.

In recording current−voltage curves using CV, the following procedure was used: 100 μL of 0.3 M stock solution of a dialdehyde in acetonitrile was added to 9.90 mL of buffer solution (phosphate, acetate, or borate), sodium hydroxide solution (for oxidations using the gold electrode) of the desired pH value, or buffer solutions of varying acetonitrile concentrations. Current−voltage curves were recorded after purging with N_2 for oxygen removal for about 2 min. The final concentration of the studied compound was 3 mM. Both electrodes (GCE and GE) were polished using 0.3 μm alumina powder, sonicated in deionized water for at least 10 min, washed with methanol, and then dried prior to use.

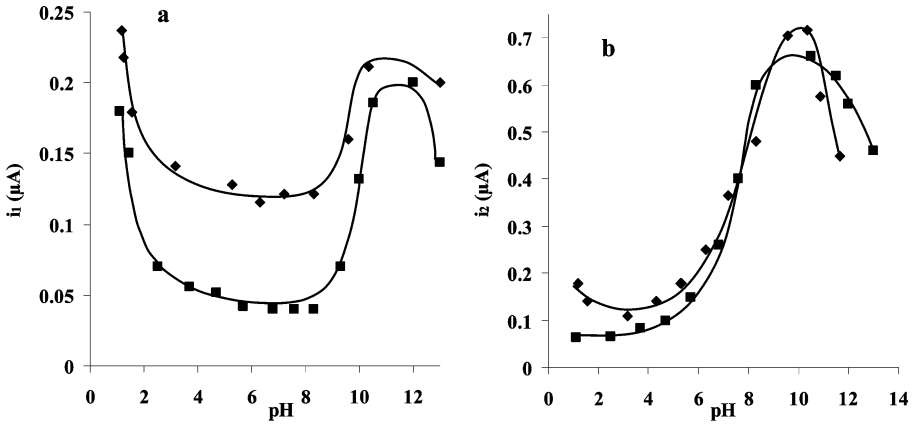

Figure 2. Dependence of the limiting current of 0.1 mM orthophthalaldehyde on pH: (a) wave i_1, (b) wave i_2. For both currents ■ corresponds to the presence of 1% acetonitrile and ◆ to the presence of 30% acetonitrile.

TABLE 1: Slopes of the pH Dependences of the Half-Wave Potentials of Polarographic (DME) Waves of 0.1 mM Orthophthalaldehyde and of Peak Potentials Obtained with the GCE of 3.0 mM Orthophthalaldehyde

[CH_3CN] (%)	pH range	d$E_{1/2}$/d(pH)	pH range	d$E_{1/2}$/d(pH)	pH range	d$E_{1/2}$/d(pH)
			DME			
			wave i_1			
1	0.0−1.6	0.0	1.6−8.5	0.045		
30	0.0−1.6	0.0	1.6−10.0	0.066	10.0−13.0	0.0
			wave i_2			
1			0.8−8.5	0.055		
30	0.0−1.7	0.0	1.7−9.5	0.060	9.5−13.0	0.0
			GCE			
			peak i_{p1}			
1	0.0−7.4	0.032	7.4−10.7	0.054	10.7−13.0	0.0
			peak i_{p2}			
1	2.0−5.0	0.049	5.5−8.0	0.139	8.0−14.0	0.0

For measurements of absorption in the UV region 0.1 mM solutions of the investigated dialdehydes were used. All solutions contained 1% acetonitrile unless otherwise indicated.

For recording of ^{1}H NMR, 14.0 mg of dialdehyde was dissolved in 1.0 mL of D_2O/CD_3CN mixtures of different compositions. Acetone solution in D_2O (14.0 mg of acetone/mL of D_2O) was used as an internal standard for monitoring the integrated areas of the studied peak. The internal standard was filled in a capillary tube, sealed, and then inserted into the NMR tube. The same internal standard was used for all ^{1}H NMR measurements throughout this work, except for ^{13}C NMR, which was performed using 14.0 mg of dialdehyde/mL of 100% CD_3CN or solutions of different CD_3CN/D_2O ratios without using an internal standard.

Results and Discussion

Polarographic Reduction of OPA takes place in two reduction waves, i_1 and i_2, as reported earlier[8] (Figure 1). Both limiting currents i_1 and i_2 are pH-dependent (Figure 2), in the presence of both 1% and 30% acetonitrile. At pH 4−8, where current i_1 is pH-independent, it is controlled by diffusion, as confirmed by dependences on the concentration, mercury pressure, and temperature (Supporting Information 1, Table S1b).

The limiting current i_1 is attributed to the reduction of the unhydrated dialdehyde (I_a) and current i_2 to the reduction of species bearing a single formyl group on the benzene ring. Both these currents in the pH range where they are pH-independent (pH 4−8 for i_1 and pH 1−3.5 for i_2) are much smaller than the limiting current of the two-electron reduction obtained in an equimolar solution of isophthalaldehyde.[10] This is attributed to a strong hydration of carbonyl groups in aqueous solutions of OPA following reaction 1.

$$I_a + H_2O \rightleftharpoons I_b \rightleftharpoons I_c \quad (1)$$

Current i_1 is attributed to a two-electron reduction of the protonated form of species I_a, which is generated from its conjugate base in the vicinity of the electrode surface in reaction 2. The slopes of the d$E_{1/2}$/d(pH) plots (Table 1) are in agreement with an irreversible electrode process involving transfer of two electrons and two protons in reactions 2 and 3. The pH at the intersection of two linear segments of the plots of $(E_{1/2})_1 = f$(pH) (Figure 3a) corresponds to a p$K_a \approx 1.6$ of reaction 2 at the electrode surface.

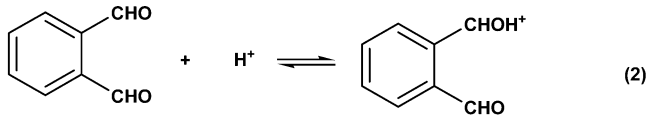

(2)

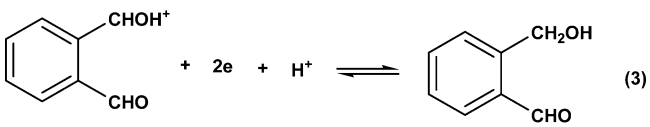

(3)

The diffusion control of current i_1 between a pH of about 4 and a pH of 8 confirms that the equilibrium, in which form I_a participates, is relatively slowly established and is not perturbed by electrolysis. Current i_1 is thus proportional to the concentra-

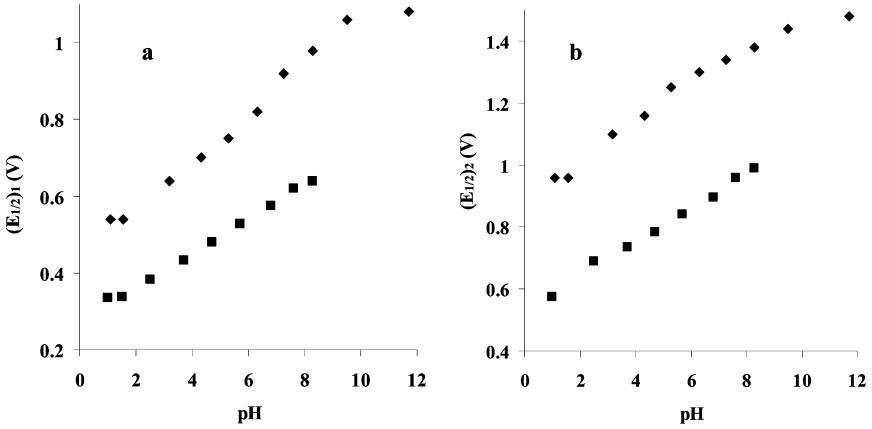

Figure 3. Dependence of the half-wave potentials of 0.1 mM solutions of orthophthalaldehyde on pH: (a) wave i_1, (b) wave i_2. For both currents ■ corresponds to the presence of 1% acetonitrile and ◆ to the presence of 30% acetonitrile.

SCHEME 1

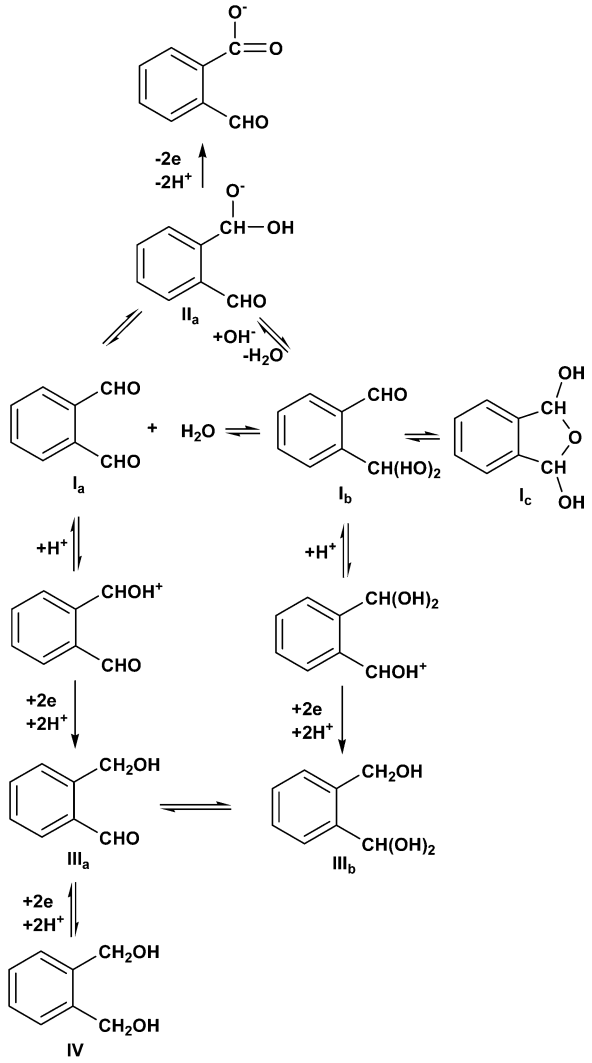

tion of form I_a at equilibrium. This can be used to estimate the equilibrium constants in reaction 1, as discussed below.

The reduction of form I_a in wave i_1 takes place at potentials about 300 mV more positive than those of wave i_2 (Figure 3), which occurs in a potential range in which most monosubstituted benzaldehydes are reduced. The shift of $(E_{1/2})_1$, which is due to the introduction of the second formyl group, is much larger than would be predicted for substituted benzaldehydes on the basis of the σ_{P-CHO} value, even taking the probability factor into

SCHEME 2

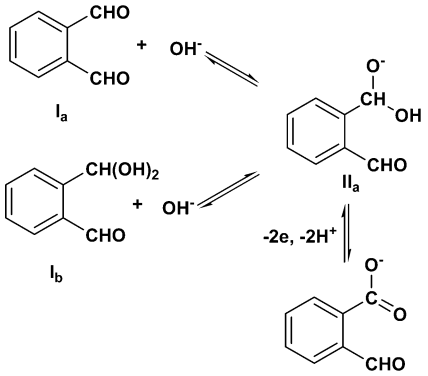

consideration. This strong facilitation of the reduction of a protonated formyl group in the presence of another formyl group as a substituent may be partly caused by a direct field or another kind of ortho effect, but may be predominantly attributed to an exceptionally strong resonance interaction between two formyl groups in ortho positions. A similar strong resonance interaction has been recently reported[11] to occur between two CHO groups in the para positions of terephthalaldehyde.

The increase in current i_1 with increasing acidity at pH < 3 (Figure 2a) is attributed to an acid-catalyzed conversion of forms I_b and I_c into the reducible form I_a. The increase of current i_1 at pH > 8 is due to a base-catalyzed conversion of forms I_b and I_c into I_a. The decrease of current i_1 at pH higher than about 10.0 is due to the formation of a geminal diol anion (II_a), either by addition of hydroxide ions to form I_a or by dissociation of the geminal diol group in form I_b (reaction 4). This is an example of a system in which two acids, one Brønsted acid (I_b) and one Lewis acid (I_a), share a common base (II_a).

$$I_a + OH^- \rightleftharpoons II_a \rightleftharpoons I_b + OH^- \quad (4)$$

The reduction process in wave i_2 is more complex. This reduction occurs in a potential range in which a two-electron reduction of most monosubstituted benzaldehydes takes place. Such a reduction of a CHO group can involve both the product (III_a, Scheme 1) of the reduction in wave i_1 and the free aldehydic group in form I_b. If wave i_2 were just a consecutive reduction of the second formyl group of the product generated in wave i_1, the ratio of i_2 to i_1 would be 1.0 and would remain pH-independent. The varying ratio i_2:i_1 (Table 2) indicates that current i_2 depends both on the concentration of the aldol III_a (product of the first reduction step of the unhydrated form (I_a)) and on the concentration of the monohydrated acyclic form (I_b).

TABLE 2: Dependence of the Ratios i_2:i_1 on pH for Currents of Reduction of Orthophthalaldehyde (OPA) Obtained by a Mercury Dropping Electrode (DME) and Glassy Carbon Electrode (GCE). Concentration of OPA Is 0.1 mM when DME Is Used and 3.0 mM for Voltammetry with GCE

DME	pH	1.1	2.5	3.7	4.7	5.7	6.8	7.6	8.3	10.5	11.5	12.0	13.0
	i_2:i_1	0.36	0.94	1.5	1.9	3.5	6.5	10	15	3.6	2.4	2.8	3.2
GCE	pH	2	3.5	4.6	5.6	7.4	7.9	9.15	9.7	10.6	11.6	12.35	
	i_{p2}:i_{p1}	0.74	0.71	1.05	1.4	8.9	9.2	6.6	4.15	2	1.5	1.84	

Thus, the difference $i_2 - i_1$ is proportional to the concentration of form I_b. The sequence of the reduction processes is indicated in the lower part of Scheme 1. This would be strictly true if the equilibria involving hydrated forms I_b and III_b were not perturbed by the electrolysis. Under such conditions the establishment of equilibria among I_b, I_a, and I_c as well as those between III_b and III_a was slow when compared to the rate of the electroreduction and if the limiting currents were purely diffusion controlled. The plot of i_2 versus $h^{1/2}$ is linear, but it does not pass through the origin (Supporting Information, Figure S2). This indicates some kinetic contribution to current i_2, which is so small that it can be, in first approximation, neglected.

Polarographic Oxidation. The decrease of both reduction currents i_1 and i_2 at pH higher than 10 (Figure 2) is accompanied by an increase of the anodic wave (i_{anod}) with increasing pH (Figure 4). With increasing activity of the hydroxide ions, the half-wave potentials of the anodic wave are shifted to more negative values by about 90 mV/pH. Similarly to that for other substituted benzaldehydes,[12] this anodic wave is attributed to an oxidation of a geminal diol anion to a carboxylate. In this case the geminal diol anion can be formed both by addition of hydroxide ions to the unhydrated dialdehyde (I_a) and by dissociation of the monohydrated acyclic form (I_b) following Scheme 2. The half-wave potential of the anodic wave becomes with increasing pH more negative and becomes pH-independent at about pH 13.3 (Supporting Information 2). This pH corresponds to the pK_a of the acid−base reaction, yielding the geminal diol anion (II_a) (Scheme 2). With decreasing pH the limiting current of the anodic wave decreases (Figure 4). The plot of $i_{anod} = f(\text{pH})$ has the shape of a dissociation curve. The pH at $i = i_d/2$, at the inflection point of the dissociation curve, which is 12.0, is denoted pK'. In accordance with the theory for anodic oxidations[12] preceded by an acid−base reaction yielding the electroactive base form, the value of pK' is smaller than the true value of pK_a.

Reduction on the GCE. The rate of acid−base reactions accompanying the reduction of OPA on the GCE resembles closely those preceding the reduction on the DME. Similarly to the reduction of OPA on the DME, the reduction on the GCE takes place in two steps, manifested by peaks i_{p1} and i_{p2}. Thus, the changes of the currents (Figures 2 and 5) and potentials, obtained by polarography and voltammetry (Table 1), follow qualitatively a similar pattern. Qualitatively, the comparison of the dependence of the currents on pH indicates that the acid-catalyzed dehydration, yielding the unhydrated form (I_a) reduced in the more positive step, plays a larger role for reductions on the DME than on the GCE. Similarly, i_{p2} corresponding to the second reduction step increases only at pH values higher than those for i_2. This indicates a smaller role of the rate of base-catalyzed dehydration on the GCE. Similarly to that of the reduction on the dropping mercury electrode, the ratio i_{p1}:i_{p2} varies with pH, which excludes a consecutive reduction (Table 2).

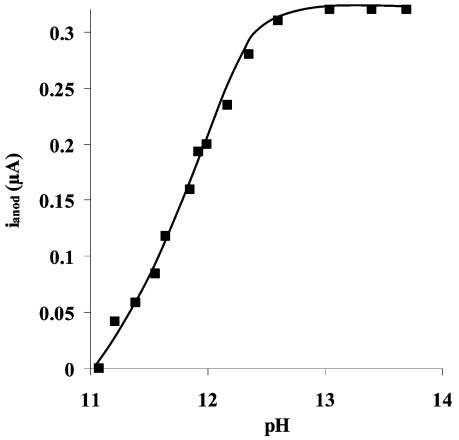

Figure 4. Dependence of the anodic limiting currents (i_{anod}) of 0.1 mM orthophthalaldehyde in 1% acetonitrile on pH in phosphate buffers (pH 11−12) and solutions of sodium hydroxide, with the ionic strength kept at $\mu = 1.0$ by addition of potassium chloride.

The pH range, in which the rate of protonation of the predominant base form becomes too slow to convert it completely into the more easily reducible conjugate acid, occurs for reductions on the GCE at higher pH values than on the DME. This pH range is characterized by the value of the pH at which potentials become pH-independent, denoted pK'' (Supporting Information 3). This pH for reduction current i_1 on the DME is equal to 10.0, and that for current i_{p1} for the reduction on the GCE is equal to 11.0 (Table 1). Similarly for the second reduction step i_2 p$K'' = 9.5$ at the DME and for i_{p2} on the GCE p$K'' = 8.0$. Greater differences at pH < 3 reflect the differences in the acid-catalyzed processes on the two electrodes used.

The analogous pattern of reduction of OPA on the DME and GCE, which is not frequently encountered, indicates that adsorption does not play a predominant role and that the role of an antecedent chemical reaction affects the currents on the GCE more than the rate of the electron transfer.

Similarly to the limiting currents obtained with DME, peak currents i_{p1} and i_{p2} are a linear function of the concentration of OPA within the whole pH range studied. Also the dependence of the measured current on temperature, as characterized by the temperature coefficient di_p/dT, is comparable for both electrodes (Supporting Information 1, Table S1a). At pH 7.4 peak current i_{p1} decreases linearly with increasing concentration of water whereas peak current i_{p2} increases (Supporting Information 4). The slopes of di/d[H_2O] were 0.93 for i_{p1} and 0.60 for i_{p2}. At pH 1−5.6 the plots of i_{p1} as a function of $\nu^{1/2}$ are linear and pass through the origin, confirming that the reduction of form I_a is diffusion controlled and the establishment of equilibrium 1 is slow relative to the rate of transport of OPA to the electrode surface by diffusion. At pH 9.15 and 10.6, plots of $i_{p1} = f(\nu^{1/2})$ are linear (Supporting Information 5), but these plots show a considerable intercept on the current axis, indicating a strong role of the rate of formation of geminal diol anion (II_a) in processes summarized in Scheme 2. The dependence of the current i_{p2} on $\nu^{1/2}$ is linear at both pH 3.5 and 9.15 (Supporting Information 5b), but the plot at pH 9.15 shows an intercept on the current axis.

Oxidation on the Gold Electrode. Polarographic investigation indicated that the form of OPA which can undergo oxidation is present only in alkaline solutions. Therefore, the investigation

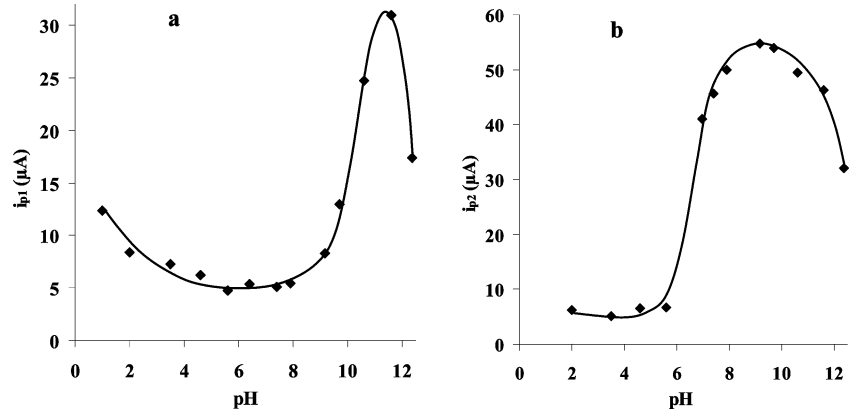

Figure 5. Dependence of voltammetric peak currents obtained with a glassy carbon electrode for reduction of a 3 mM solution of orthophthalaldehyde on pH in the presence of 1% acetonitrile: (a) peak i_{p1}, (b) peak i_{p2}.

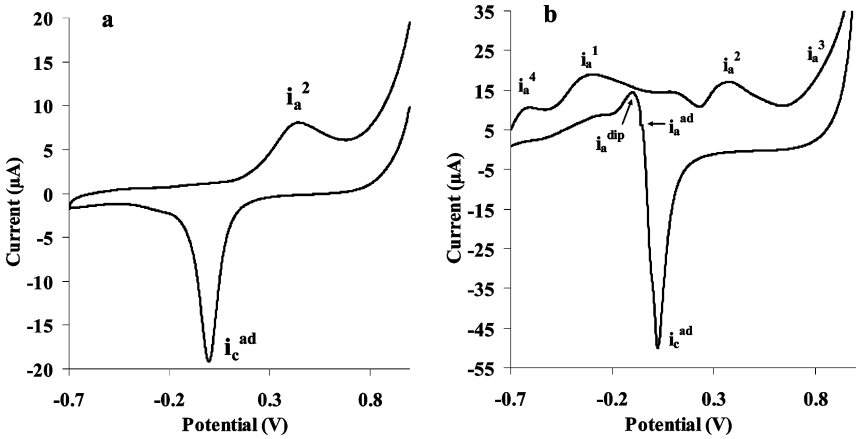

Figure 6. Cyclic voltammograms in 0.5 M NaOH containing (a) 0 and (b) 3 mM orthophthalaldehyde on a gold electrode (initial potential 1.0 V, switching potential −0.7 V).

of the oxidation of OPA using the gold electrode was restricted to strongly alkaline solutions. Under these conditions, oxidation of the gold electrode can take place and the resulting gold cations can interact with hydroxide ions. To distinguish processes due to oxidation of the gold electrode from peaks on $i-E$ curves due to oxidation and/or adsorption of OPA, it was first necessary to record $i-E$ curves obtained with the gold electrode in solutions containing only sodium hydroxide (Figure 6a). For an elucidation of electrode processes involving organic compounds, the understanding of the role of the activities of H^+ or OH^- ions is often important. In the existing experimental evidence[13] limited attention has been paid to this aspect. It was thus necessary to record first $i-E$ curves using the gold electrode in solutions of varying concentrations of sodium hydroxide with some control of the ionic strength. On $i-E$ curves, obtained in such solutions, were observed three current peaks, one cathodic peak (i_c^{ad}) and two anodic peaks (i_a^2 and i_a^3) (Table 3). The most positive peak i_a^3 was observed only at the highest concentration of hydroxide ions. The cathodic peak i_c^{ad} is controlled by adsorption. This was proved by a nonlinear dependence of the peak currents on the scan rate (ν). In this peak gold ions are reduced. These ions are released from compounds resulting from the interaction of gold ions with hydroxide ions, which will be further denoted as complexes, that are slightly soluble. The gold ions needed in formation of this complex are formed by electrooxidation of the gold electrode after it is immersed into an alkaline solution. The release of gold ions from the adsorbed layer of the complex is not extremely fast. This is indicated by the round shape of peak i_a^2, which is also limited by adsorption. The change in the shape of the peak indicates that the rate of the release of gold ions increases with increasing concentration of hydroxide ions. The formation of slightly soluble compounds or complexes resembles that observed at mercury electrodes[14] in alkaline media, where nevertheless the equilibria between the adsorbed complex and mercury ions are more rapidly established. Available experimental evidence does not allow distinguishing between the oxidation states of gold in complexes formed nor does it offer information about the number of hydroxide ions in such complexes. The limited solubility of such complexes, nevertheless, indicates that the complexes formed do not bear any charge.

Peak i_a^2 is observed at potentials about 0.35 V more positive than those of peak i_c^{ad} (Table 3). The difference between E^a_{p2} and E^c_{ad} is practically pH-independent. The shapes of plots of $i_a^2 = f([OH^-])$ and $i_a^2 = f(\nu)$ indicate that the formation of the adsorbed layer is fast (Table 4). Available experimental evidence does not allow us to decide whether the compositions of the complexes adsorbed in i_c^{ad} and i_a^2 are identical. Similar shapes of $dE_{1/2}/d(pH)$ plots (72 mV/pH for i_c^{ad} and 78 mV/pH for i_a^2) (Supporting Information 6) nevertheless indicate formation of similar complexes. The large difference of about 0.35 V between the potentials of i_c^{ad} and i_a^2 may be attributed to differences in the structures of the adsorbed layer or control of the adsorption−desorption equilibria by kinetic factors.

Peak i_a^3, observed with gold electrodes only at the highest concentrations of OH^- ions at the most positive potentials, also corresponds to an oxidation of the gold electrode and formation of another slightly soluble complex of gold ions with hydroxide ions. The dependence of $i_a^3 = f([OH^-])$ (Table 4) indicates that the resulting adsorbed layer is rapidly formed. At present it is

TABLE 3: Dependence of the Peak Currents and Potentials in a 3.0 mM OPA Solution on the Acidity of an Alkaline Solution[a]

peak	pH (J^-) 11.5	pH (J^-) 12	pH (J^-) 13	pH (J^-) 13.8	pH (J^-) 14.5	pH (J^-) 14.9	pH (J^-) 15.3
				peak currents			
i_a^3				5.7	13.7[b]	47.0[b]	43.0[b]
						(23.0)[c]	(14.7)[c]
i_a^2	3.2	2.5	1.5	5.3	14.0[b]	20.0[b]	23.4[b]
	(4.7)[c]	(3.7)[c]	(6.0)[c]	(9.0)[c]	(10.2)[c]	(13.0)[c]	(12.6)[c]
i_c^{ad}	14.8	11.8	15.6	24.6	50.0[b]	82.0[b]	84.7[b]
	(14.0)[c]	(14.0)[c]	(18.0)[c]	(28.6)[c]	(27)[c]	(37.0)[c]	(20.6)[c]
i_a^{ad}			17.3	16.3			
i_a^{dip}	24.0	23.8	32.0	33.0	37.6[b]	33.0[b]	25.0[b]
i_a^1			9.5	9.8	13.7[b]	15.0[b]	8.6[b]
i_a^4	9.0	9.0	7.3	5.0	3.20		
				peak potentials			
i_a^3				0.85	0.78	0.78	0.74
						(0.78)[c]	(0.78)[c]
i_a^2	0.57	0.50	0.42	0.39	0.29	0.29	0.27
	(0.59)[c]	(0.51)[c]	(0.47)[c]	(0.40)[c]	(0.28)[c]	(0.26)[c]	(0.27)[c]
i_c^{ad}	0.18	0.15	0.07	0.02	−0.045	−0.07	−0.08
	(0.17)[c]	(0.13)[c]	(0.07)[c]	(0.03)[c]	(−0.033)[c]	(−0.041)[c]	(−0.052)[c]
i_a^{ad}			0.04	−0.02	−0.12		
i_a^{dip}	0.13	0.11	−0.02	−0.08	−0.12	−0.16	−0.18
i_a^1			−0.21	−0.29	−0.39	−0.46	−0.52
i_a^4	−0.51	−0.55	−0.6	−0.64	−0.64		

[a] Characterized by pH or acidity function J^-. Data obtained in the absence of OPA in sodium hydroxide solutions are given for comparison in parentheses. [b] Corrected for the effect of viscosity. [c] Data for a solution of sodium hydroxide in the absence of OPA. Subscript "a" corresponds to anodic current, subscript "c" corresponds to cathodic current, and subscript "ad" corresponds to adsorption current.

TABLE 4: Voltammetry of 3 mM Solutions of Orthophthaldehyde on a Gold Electrode in Solutions of Sodium Hydroxide

current	species[a]	type of process[b]	$dE_p/d(pH)$ (V/pH)		type of process[c]
i_a^3	OH^-	fast adsorption	−0.070	$i = f(\nu)$	adsorption
i_a^2	OH^-	fast adsorption	−0.078	$i = f(\nu)$	adsorption
i_c^{ad}	OH^-	slow adsorption	−0.072	$i = f(\nu)$	adsorption
i_a^{ad}	OPA	diffusion	−0.100	$i = f(\nu^{1/2})$	diffusion
i_a^{dip}	OPA	diffusion or kinetic	−0.085	$i = f(\nu^{\circ})$	kinetic
i_a^1	OPA	diffusion	−0.136	$i = f(\nu^{1/2})$	diffusion

[a] Electroactive species. [b] In 0.5 M NaOH, $J^- = 13.8$, from $i = f(c)$. [c] From $i = f(\nu)$.

not possible to distinguish whether the compound formed in i_a^3 differs from that formed in i_a^2 by the oxidation state of gold, by the composition of the slightly soluble compound formed, or by the difference in the structure of the adsorbed layer.

Addition of OPA to solutions of sodium hydroxide did not practically affect the potentials of peaks i_c^{ad}, i_a^2, and i_a^3 (Table 3) observed in the absence of OPA. At lower concentrations of hydroxide ions currents i_c^{ad}, i_a^2, and i_a^3 varied in the presence of OPA only slightly. Only at $J^- > 14$, where OPA is predominantly present in an anionic form, all three peak currents increased markedly (Table 3). This indicates that the presence of the anionic form of OPA affects the composition of the adsorbed layer, for example, by inclusion of anions of OPA. Currents i_a^{ad}, i_a^{dip}, and i_a^1, observed only in the presence of OPA (Figure 6b), are a linear function of the concentration of OPA (Supporting Information 7). They correspond to the oxidation of the geminal diol anion of OPA (II_a) which is present in alkaline solutions. Peak currents i_a^{ad} and i_a^1 are linear functions of $\nu^{1/2}$ and are thus diffusion controlled. Current i_a^{dip} is independent of the scan rate (ν), which indicates control by the rate of a chemical reaction, possibly by the rate of establishment of equilibria involved in formation of the geminal diol anion. Peak current i_a^1 increases with increasing concentration of hydroxide ions. The shape of the plot of $i_a^1 = f(J^-)$ (Figure 4) indicates that the electrooxidation, taking place on an adsorbed layer of the complex, is preceded by a chemical reaction, such as formation of the geminal diol anion of OPA formed in the reaction of OPA with OH^- ions (see below).

Absorption Spectra of OPA and isomeric benzenedicarboxaldehydes in the UV region show three main absorption bands: one at about 220 nm corresponding to various π to π^* transitions, the second in the region between 240 and 270 nm due to the π to π^* transitions involving the aromatic π-electrons and those electrons of the double bonds conjugated with the aromatic ring, and a third between 290 and 310 nm attributed to the forbidden n to π^* transition involving π-electrons of the carbonyl group. For all transitions the wavelengths of the absorption maxima in dioxane and water agreed within ±3 nm (Table 5). For IPA and TPA molar absorptivities of the benzoyl groupings are similar in acetonitrile and dioxane, as found for the absorptivities corresponding to the n to π^* transition (considering for IPA the sum of absorbances at 290 and 299 nm). Lower values of ϵ observed for such absorption in acetonitrile solutions can be ascribed to traces of water. This is supported by higher molar absorptivities, obtained for aqueous solution, when the absorbance was extrapolated to $t = 0$ (Table 5).

The molar absorptivities of dialdehydes at about 300 nm—in the absence of hydration—are more than 40% higher than those of other substituted benzaldehydes. This reflects the statistical factor, due to the increased probability of excitation of electrons of the two formyl groups. The wavelength of the carbonyl group absorption in benzaldehyde is in the presence of the second formyl group shifted by 10−15 nm to longer wavelength, due to the introduction of an electron-withdrawing substituent. The absorbance at 210−220 nm can be affected by too many types of transitions to allow interpretation. The π to π^* and n to π^* transitions at about 260 and 300 nm remain comparable between pH 3 and about pH 10. At higher pH values they decrease with increasing pH, and plots of $A = f(\text{pH})$ have the shape of an acid dissociation curve with $pK_a^{exp} = 12.1$ at 301 nm and 12.8 at 260 nm (Figure 7). This acid−base equilibrium corresponds to Scheme 2. Equilibrium concentrations of I_a and I_b in alkaline media, corresponding to the equations $K_a^1 = [II_a]/[I_a][OH^-]$ and

TABLE 5: UV Absorption of Benzaldehyde and Benzenedicarboxaldehydes (λ, nm; ϵ, L mol^{-1} cm^{-1})

compound	solvent	λ_1	$\epsilon \times 10^4$	λ_2	$\epsilon \times 10^4$	λ_3	$\epsilon \times 10^3$
benzaldehyde	CH_3CN			244	1.63	289	1.26
	1,4-dioxane[a]			250	1.40	282	1.60
orthophthalaldehyde	CH_3CN	219	2.13	260	0.56	301	1.54
	1,4-dioxane[a]	222	1.70	263	0.85	297	2.20
	H_2O[b]	221	3.40	262	1.10	301	3.60
	H_2O[c]	221	0.60	262	0.22	301	0.80
isophthalaldehyde	CH_3CN	225	0.45	243	1.40	301	1.12
	1,4-dioxane[a]	224	3.00	248	1.30	299	1.00[d]
terephthalaldehyde	CH_3CN			258	2.11	301	1.88
	1,4-dioxane[a]			261[e]	2.10	296	2.10

[a] Data from ref 6. [b] Extrapolated to time 0. [c] Values at equilibrium. [d] Additional band at 290 nm, $\epsilon = 1.01 \times 10^3$ L mol^{-1} cm^{-1}. [e] Additional shoulder at 266 nm, $\epsilon = 1.58 \times 10^4$ L mol^{-1} cm^{-1}.

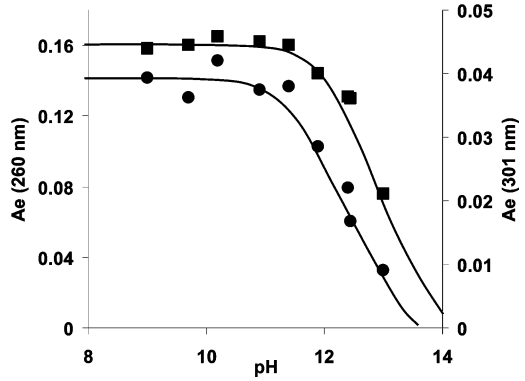

Figure 7. Dependence of the absorbance in a solution of 0.1 mM orthophthalaldehyde on pH: absorbance at 260 nm, ●, left-hand scale, and at 301 nm, ■, right-hand scale.

$K_a^2 = [II_a]/[I_b][OH^-]$, are not known with sufficient accuracy. Their separation using the expression $pK_a^{exp} = pK_a^1 + pK_a^2 + \log(K_a^1 + K_a^2)$ is not possible. With increasing temperature the absorbances at both 260 and 300 nm increase (Supporting Information 8).

NMR Spectra of 0.1 M OPA and 0.1 M IPA were compared in a solution containing 65% D_2O and 35% CD_3CN. For solutions of OPA the following signals were observed: The signal at $\delta = 6.57$ (integrated area 0.43) is attributed to the CH protons of the hemiacetal ring in form I_c. The signal at $\delta = 6.9$ is due to the CH proton in the geminal diol group of the form I_b (integrated area 0.35) and the signal at $\delta = 10.75$ (integrated area 0.24) to the protons in the formyl groups in forms I_a and I_b. Multiplet signals at $\delta = 7.7$, 7.93, and 8.1 are attributed to the aromatic protons. In solutions of IPA, which is practically not hydrated, the signal at $\delta = 10.75$ (integrated area 0.84) is due to the protons of the free formyl groups.

Reaction of OPA with Water. Equilibria. In reported investigations[6] of the equilibria in reaction 4a by spectrophotometry, it was assumed that the concentration of I_b at

$$I_a + H_2O \underset{K_1}{\rightleftharpoons} I_b \underset{K_2}{\rightleftharpoons} I_c \qquad (4a)$$

equilibrium was negligible. The presence of form I_b escaped attention, because in the region between 250 and 280 nm absorption bands of form I_b are overlapped by those of form I_a, which has a higher molar absorptivity than form I_b. This is caused by the less extended conjugation of the single carbonyl group in I_b as compared to two such groups in I_a. Furthermore, the absorption bands of I_b, due to a $\pi \rightarrow \pi^*$ benzenoid transition, are overlapped also by absorption bands due to the benzene ring in I_c. The latter have a lower molar absorptivity due to a lack of conjugation with the side chain, but are present at a concentration of I_c almost an order of magnitude higher than that of form I_b. This situation prevents determination of individual equilibrium constants K_1 and K_2 by measurements of absorbances. To characterize the equilibria in reaction 4a using spectrophotometry, it is possible—as a first approximation—to neglect the contribution of form I_b to the measured absorbances. This together with the assumption that the absorbance at 300 nm is only due to form I_a makes it possible to obtain an overall constant $K'_H = ([OPA]_o - [I_a]_e)/[I_a]_e[H_2O]$. The conversion of concentrations in this expression would involve the knowledge of the molar absorptivity of OPA in water, which is not directly accessible. Two approaches were used as approximations: In the first approach the absorbance of OPA in water was considered practically equal to the absorbance of an equimolar solution of OPA in acetonitrile ($A^{OPA}{}_{CH_3CN}$). Then $K'_H = (A^{OPA}{}_{CH_3CN} - A^{OPA}{}_e)/(A^{OPA}{}_e[H_2O])$. In the second approach the assumption was made that the molar absorptivity of unhydrated OPA in water is practically equal to that of IPA, which is less than 3% hydrated. This leads to the expression $K'_H = (A^{IPA} - A^{OPA}{}_e)/(A^{OPA}{}_e[H_2O])$, where A^{IPA} is the absorbance of an equimolar solution of IPA in water. Another possible approach, based on extrapolation (to zero time) of the absorbances after addition of a nonaqueous solution of OPA to water, involves—in addition to the above-discussed overlap—considerable uncertainties due to the high rate of hydration.

TABLE 6: Overall Hydration Equilibrium Constants $K'_H = (A^{IPA} - A_e{}^{OPA})/(A_e{}^{OPA}[H_2O])$

solution	temp (°C)	wavelength 220 nm		wavelength 260 nm	wavelength 300 nm
H_2O	20		0.13[b]	0.14[b]	0.03[b]
	25	0.08[a]	0.09[b]	0.05[b]	0.04[b]
	40		0.07[b]	0.08[b]	0.004[b]
	60		0.035[b]	0.04[b]	
	80		0.02[b]	0.03[b]	
acetate buffer (pH 4.15)	25	0.28[a,c]	0.31[b,c]	0.14[a]	
phosphate buffer (pH 6.2)	25	0.12[a]	0.15[b]	0.06[a]	0.01[a]
borate buffer (pH 8.3)	25	0.14[a]	0.17[b]	0.08[a]	0.14[a]

[a] Comparison with the absorbance of OPA in 100% CH_3CN. [b] Comparison with the absorbance of IPA in water. [c] Affected by the absorption of CH_3COO^-.

The values of K'_H based on absorbances at 220 and 260 nm (Table 6) are in acceptable agreement, with the exception of the value of K'_H obtained using the absorbance at 220 nm in an acetate buffer (pH 4.15), which is affected by the absorption due to the acetate anion.[15] Considerable variation of K'_H values based on the absorbance at 300 nm reflects the role of the $n \rightarrow \pi^*$ transition involving the free carbonyl group in form I_b. Thus, the most reliable values of K'_H are based on the $\pi \rightarrow \pi^*$

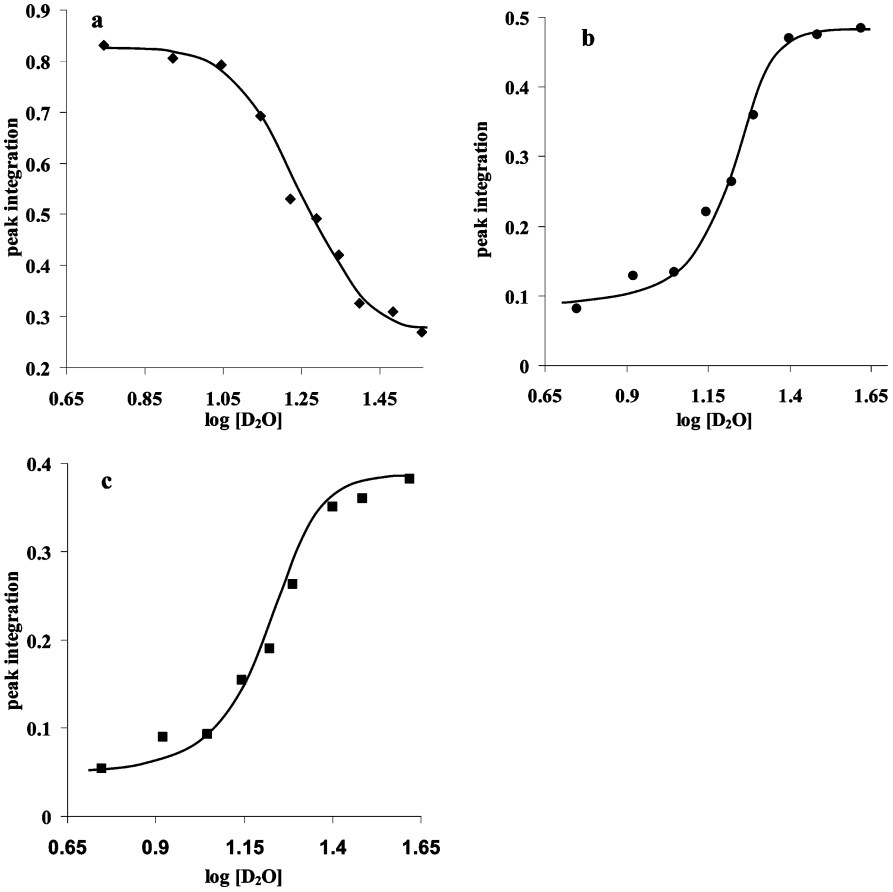

Figure 8. Dependence of the integrated area of ^{1}H NMR signals after establishment of equilibria on the concentration of D_2O in mixtures of CD_3CN and D_2O: surface area of signals at (a) $\delta = 10.75$, (b) $\delta = 6.9$, and (c) $\delta = 6.57$.

benzenoid transitions. The contribution of the absorbance due to the aromatic ring in form I_c can be neglected, due to the absence of a ring−side chain conjugation. Difference between the values of K'_H in water and in buffers (Table 6) reflects the effect of the ionic strength on the equilibria in reaction 4a.

From measurements of polarographic waves i_1 and i_2 it is possible to estimate the concentrations of forms I_a and I_b. From the known initial concentration of OPA it is thus possible to determine the concentration of I_c. At equilibrium, i_1^e is proportional to $[I_a]_e$ and $i_2^e - i_1^e$ to $[I_b]_e$. As the initial concentration of OPA ($[I]_o$) equals $[I_a]_e + [I_b]_e + [I_c]_e$, it follows that the concentration $[I_c]_e = [I]_o - ([I_a]_e + [I_b]_e)$. Since the two-electron wave of the unhydrated isophthalaldehyde (IPA), i_{IPA}, is proportional to $[I]_o$, then $[I_c]_e$ is proportional to $i_{IPA} - i_2^e$. It follows that both K_1 and K_2 can be obtained from polarographic data, as $K_1 = (i_2^e - i_1^e)/i_1^e[H_2O]$ and $K_2 = (i_{IPA} - i_2^e)/(i_2^e - i_1^e)$ (Supporting Information 9).

The overall equilibrium constant K'_H can also be estimated from the dependence of the NMR spectra on the concentration of D_2O in a mixture with CD_3CN. With increasing concentration of water the integrated area of the signal at $\delta = 10.75$ decreases (Figure 8a). This decrease is accompanied by an increase in the integrated areas of signals at $\delta = 6.9$ of the CH protons of form I_b and at $\delta = 6.57$ due to the hemiacetal ring protons (Figure 8b,c). The plots of the peak area as a function of log $[D_2O]$ have the shape of a dissociation curve, for $\delta = 10.75$ decreasing and for both signals $\delta = 6.57$ and 6.9 increasing. All three dissociation curves have an inflection point at log $[D_2O] = 1.25$ that corresponds to $pK'_H = 1.25$ in a mixture of 25% D_2O and 75% CD_3CN. The corresponding value $K'_H = 0.056$ is comparable with values of K'_H obtained at 25 °C in unbuffered aqueous solutions (Table 6). Attribution[6b] of the signals at $\delta = 6.21$ and $\delta = 6.61$ to *cis*- and *trans*-cyclic forms of I_c is doubtful. The claim of these authors that[6b] the two peaks merge with increasing temperature could not be verified; actually these peaks remained well separated up to 80 °C.

The use of currents i_1 and i_2 for the estimate of $[I_a]_e$ and $[I_b]_e$ is limited to the pH range where these currents are pH-independent and where the rate of the acid- and base-catalyzed dehydration is negligible. This condition is fulfilled (Figure 2) at pH between 4 and 8 for i_1 and pH between 1 and 3.5 for i_2. In these pH ranges, the average current i_1 in a 0.1 mM solution of OPA is 0.05 μA, that of i_2 is 0.11 μA, and the current of the two-electron reduction of IPA is 0.85 μA at 25 °C. This yields in solutions containing 1% acetonitrile at 25 °C values $K_1 = 0.02$ mol·L^{-1} and $K_2 = 9.9$. Hence, $K_H = K_1K_2 = 0.25$, which is higher than the value 0.12 obtained for K'_H in a buffer of pH 6.2 (Table 6). Due to ill-separated peaks i_{p1} and i_{p2} of OPA and ill-developed peaks in solutions of IPA at pH 3.5 in CV on a glassy carbon electrode, the corresponding peak currents were not used for evaluation of equilibrium constants.

On the basis of measurements of UV spectra and comparison with the absorbance of an equimolar solution of IPA, it was possible to obtain values of K'_H in mixtures of water with acetonitrile. The values of K'_H decrease with decreasing water content (Table 7). Thus, in unbuffered aqueous solutions OPA was present at about 88% in form I_c, but in a solution containing 30% acetonitrile with 70% water the concentration of form I_c is only about 53%. Attribution of the increase of the value of K'_H with increasing water concentration in mixtures with an organic solvent to the solvent effect[6] does not seem plausible. The dependence of K'_H on the water content was further

TABLE 7: Dependence of the Overall Constant K'_H of the Reaction of 0.1 M OPA with Water on the Concentration of Water in a Mixture with Acetonitrile[a]

$[H_2O]$ (%)	97.2	92.5	90	80	70	60	50
K'_H(260 nm)	0.06	0.06	0.06	0.04	0.03	0.04	0.03
K'_H(301 nm)	0.10	0.08	0.08	0.03	0.02	0.04	0.05

[a] K'_H was obtained by using the absorbance at 262 nm, compared to the absorbance of an equimolar solution of IPA in an unbuffered system.

TABLE 8: Dependence of Equilibrium Constants K_1, K_2, and K_H for the Reaction of 0.1 mM OPA with Water in a Phosphate Buffer (pH 3.45) on Temperature

T (°C)	23	33	40	50
K_1 (mol^{-1} L)	0.021	0.016	0.017	0.011
K_2 (mol^{-1} L)	9.9	7.2	5.3	4.9
K_H (mol^{-1} L)	0.21	0.11	0.09	0.05

TABLE 9: Dependence of the Rate Constant for the Establishment of Equilibria between 1×10^{-4} M OPA and Water at 25 °C on the Concentration of Water in Mixtures with Acetonitrile

$[H_2O]$ (%)	97.5	92.5	90	85	70	50	30
k_{obs}(262 nm) $\times 10^3$ (s^{-1})	2.8	1.8	1.6	1.4	1.4	0.7	0.5
k_{obs}(301 nm) $\times 10^3$ (s^{-1})	2.3	1.8	1.6	1.4	1.4	0.7	0.5
$[H_2O]$ (M)	54	51	50	47	39	28	16.7
k_{H_2O}[a] $\times 10^5$ (L mol^{-1} s^{-1})	5.2	3.5	3.2	3.0	3.6	2.5	3.0

[a] $k_{H_2O} = k_{obs}/[H_2O]$.

attributed[6b] to the interaction of two water molecules with a molecule of OPA. Such an interaction can play a role in formation of a transition state, but not in established equilibria. The observed variation in K'_H (Table 7) can be more probably attributed to a decrease in the activity of water due to solvation by acetonitrile.

The dependence of polarographic limiting currents i_1 and i_2 on temperature (Supporting Information 1, Table S1a) enables determination of equilibrium constants K_1, K_2, and K_H at various temperatures (Table 8). With increasing temperature the equilibria are shifted in favor of the acyclic forms I_a and I_b. The plot of log K_H as a function of $1/T$ is linear.

Kinetics of Hydration. The rate of addition of water to OPA (followed by the time dependence of absorbance at both 262 and 301 nm) has been studied in unbuffered and buffered solutions. The first-order rate constant k_{H_2O} found for unbuffered aqueous solutions was in acceptable agreement with data reported earlier[6] (Supporting Information 10). In mixtures of water and acetonitrile the first-order rate constants of hydration decreased gradually with decreasing water concentrations (Table 9). The relatively small variation of the second-order rate constant $k_{H_2O} = k_{obs}/[H_2O]$ indicates that, even in these solutions containing a high molarity of water, the solvent effect is not predominant.

The spectrophotometric studies offer information about the rate of the slowest step in the establishment of equilibria among forms I_a, I_b, and I_c. They do not allow obtaining information about the rates of establishment of individual equilibria. Such information was obtained from ^1H NMR spectra in mixtures of CD_3CN and D_2O. In such solutions, containing 0.1 M OPA, it was possible to follow changes in the concentration of individual components with time. The decrease in the integrated peak areas with time enabled following the changes in concentration of form I_a using the changes in the integrated surface areas of the peak at $\delta = 10.75$ taking into consideration the contribution from form I_b. Similarly, the increase in the surface area of the peak at $\delta = 6.9$ enabled following concentration changes of form I_b and of form I_c at $\delta = 6.57$. In both studied solution mixtures (containing 50% and 20% D_2O) the total integrated area remained constant. This indicates that in the process of hydration only products I_b and I_c are formed. In both mixed solvents used, the decrease in concentration of form I_a, the increases in the concentrations of form I_a, and the increases in those of forms I_b and I_c follow first-order kinetics. The rate constant k_{obs} for the decrease in $[I_a]$ was 8.8×10^{-4} s^{-1}, for the increase in $[I_b]$ it was 6.0×10^{-4} s^{-1}, and that of the increase in $[I_c]$ was 5.5×10^{-4} s^{-1}. Larger differences in the rates of formation of I_b and I_c were observed in solutions containing 20% D_2O and 80% CD_3CN, where the hydration was so slow that the initial zero kinetics persisted at 25 °C over 200 min. In this reaction mixture where at equilibrium only about 15% of I_a has been converted, the rate constant for the conversion of form I_a was 1.7×10^{-3} min^{-1}, the rate constant of formation of form I_b was $k_{obs} = 7 \times 10^{-4}$ min^{-1}, and that for formation of I_c was $k_{obs} = 4 \times 10^{-4}$ min^{-1}. This observation further confirms the conclusion, reached above, that the signals with $\delta = 6.57$ and with $\delta = 6.9$ correspond to two species in equilibrium, rather than two isomers, as assumed before.[6]

TABLE 10: Comparison of the Rate Constants of the General-Base-Catalyzed Hydration of Orthophthalaldehyde Obtained by Measuring the Absorbance at 262 nm and by Following the Decreases of Polarographic Currents i_1 and i_2 with Time

buffer	pH	measurement	k_0[a] (s^{-1})	k_B[b] (s^{-1})	ref
acetate	4.56	A_{263}	7.8×10^{-3}	6.0×10^{-2}	6
acetate	5.63	A_{263}	6.0×10^{-3}	8.0×10^{-2}	6
acetate	4.90	A_{262}	4.1×10^{-3}	14.0×10^{-2}	this study
acetate	4.70	i_1	1.9×10^{-3}	2.0×10^{-2}	this study
		i_2	1.2×10^{-3}	1.0×10^{-2}	this study

[a] k_0 from the equation $k_0 + k_b[B]$. [b] k_b from the same equation.

The first-order kinetics of hydration in buffered solution (Supporting Information 11) is general-acid−base-catalyzed, as reported earlier.[6] Both the observed shape of the pH dependence of the first-order rate constant and the values of the rate constants for the establishment of equilibria in individual buffers reported here were acceptably close to the values in ref 6 (Supporting Information 12 and 13). The values of the first-order rate constants obtained by measuring the decrease of the absorbance at 212, 262, and 301 nm have shown a very good agreement. Rate constants obtained using decreases of limiting currents i_1 and i_2 with time were of the same order of magnitude as the values obtained by measurements of the absorbance (Table 10).

Polarography has also been used to demonstrate the chemical reversibility of the addition of water to OPA involving forms I_a, I_b, and I_c. To carry out this proof, a sample of OPA was added successively to buffers of pH 7.8, 9.3, and 10.5. After establishment of the equilibrium, to each of theses buffers was added acetic acid to adjust the pH to 4.7. Current−voltage curves recorded in such solutions were found to be qualitatively and quantitatively identical with curves obtained after addition of OPA directly to an acetate buffer (pH 4.7).

Rate of Dehydration. For a compound that can exist in aqueous solutions in two forms in equilibrium, electrochemistry enables determination of the rate constants for the formation of the electroactive species, provided that the value of the equilibrium constant is known. Measurement of polarographic limiting currents enables determination of the rate constants of the chemical reactions, by which the electroactive form is generated. This reaction takes place in the vicinity of the electrode surface in a volume of solution called the reaction layer.

Following the rate of such chemical reactions, on the basis of recorded currents, is possible, if the rate of the electrolysis

is comparable to the rate of reestablishment of the chemical equilibrium, perturbed by the reduction or oxidation of the electroactive form. Under such conditions some of the predominant electroinactive form, transported to the electrode by diffusion, is converted into the electroactive form. The rate of the chemical reaction then controls the limiting current of the electroactive species.

Examples of reduction currents, controlled by the rate of the chemical reaction, are reductions of some weak acids. As a rule, the conjugate acid is reduced at more positive potentials than the conjugate base. In such systems, the rate constant of the protonation can be determined. Other examples are the reductions of compounds present in aqueous solutions in hydration−dehydration equilibria. In such systems, reduction of the unhydrated form occurs at much more positive potentials than that of the hydrated one. For such compounds the rate constant of dehydration can be determined.

An example of a chemical reaction, preceding electrooxidation, is the behavior of some aldehydes in alkaline solutions.[12] In these cases the current is controlled by the rate of formation of the geminal diol anion, which is the electroactive oxidized form (as will be discussed below).

In solutions of OPA the current i_1, corresponding to the reduction of the unhydrated form I_a, remains pH-independent in the range between pH 4 and pH 8 (Figure 2). This current is controlled by diffusion (cf. the section on the polarography of OPA above). This indicates that in this pH range the equilibrium between the hydrated and unhydrated forms is so slowly established that it is not perturbed by electrolysis. Polarography is thus not suitable for determination of the rate constant of the solvent-catalyzed dehydration in this pH range. At pH < 3 the rate of dehydration is acid-catalyzed, as indicated by the increase in limiting current i_1 with decreasing pH. The base catalysis, on the other hand, is manifested by the increase of the current with pH increasing from 9.0 to 10.5. The investigation at pH > 10.5 is prevented by the competing formation of a geminal diol anion (see below).

The rate constants of the acid-catalyzed dehydration at pH < 3 and at pH 9−10.5 of the base-catalyzed dehydration were calculated using the equation[12] $i_k/i_d = 0.81(K'_H k_d t_1)^{1/2}/[1 + 0.81(K'_H k_d t_1)^{1/2}]$, where i_k is the measured kinetic current of the reductions of the unhydrated form of OPA, i_d the theoretical diffusion current of OPA, K'_H the equilibrium constant for the hydration−dehydration reaction, k_d the rate constant of dehydration, and t_1 the drop time.

The value of i_d for the reduction of OPA is not directly accessible due to the hydration. As a good approximation in this study the limiting current of the two-electron reduction of isophthalaldehyde,[10] which remains in aqueous solutions in the unhydrated form, was used. The constant K'_H equals the ratio of the sum of the concentrations of hydrated forms I_b and I_c to the unhydrated form I_a. As $[I_b] \ll [I_c]$ the value of K'_H practically corresponds to the equilibrium $I_a + H_2O \rightleftharpoons I_c$.

For the acid-catalyzed reaction at pH 1.1−2.45 a mean value $K'_H = 0.34$ was used to calculate the values of k_d at individual pH values. In this pH range the rate of dehydration is specific-acid-catalyzed, as demonstrated by the independence of the limiting currents (and hence k_d) of the buffer concentration. The value of k_d hence equals $k_{H_2O} + k_{H^+}[H^+]$. A linear plot of k_d as a function of $[H^+]$ (Supporting Information 14) yielded $k_{H^+} = 2.1$ L mol^{-1} s^{-1} and $k_{H^2O} = 2.2 \times 10^{-2}$ s^{-1}.

For the base-catalyzed reaction between pH 9.3 and pH 10.3, where the value $K'_H = 0.27$ was used, it was also proved that the reaction is specific-base-catalyzed, as the currents i_1 were independent of the buffer kind and concentration. In this pH range the value of $k_d = k_{H_2O} + k_{OH^-}[OH^-]$. A linear plot of $k_d = f([OH^-])$ yielded $k_{OH^-} = 7.3 \times 10^2$ L mol^{-1} s^{-1} and $k_{H_2O} = 0.5 \times 10^{-2}$ s^{-1}. The difference between the values of k_{H_2O} obtained for the acid-catalyzed and for the base-catalyzed reactions is within the limits of accuracy of the used treatment.

SCHEME 3

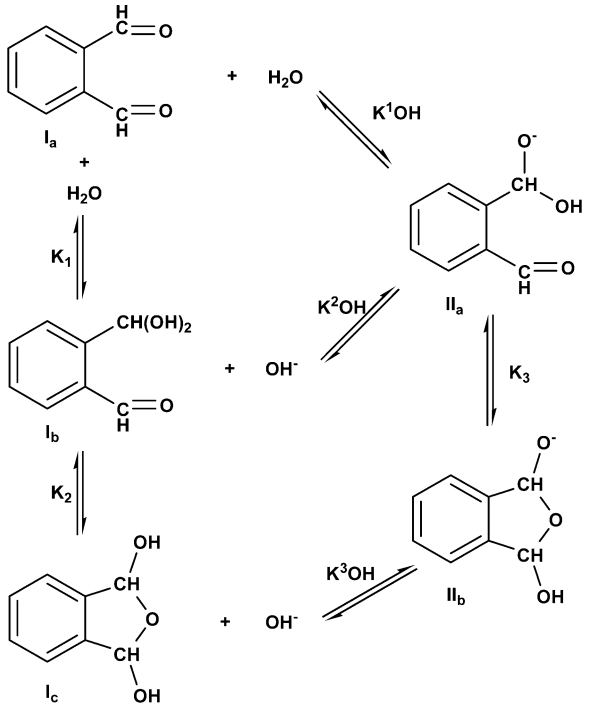

Reaction with Hydroxide Ions. Considering possible acid−base equilibria of the cyclic hemiacetal form (I_c), processes that can take place in alkaline media are summarized in Scheme 3. Earlier reports attributed the decrease of absorbance at 260 nm[6a] and 300 nm[6a,b] to a dissociation of one OH group in the cyclic hemiacetal (I_c). For the pK_a value assumed to be pK_{OH} were reported values of 11.6 at 25 °C[6a] and 12.08 at 20 °C.[6b] Our measurements showed agreement with these reports (pK_a = 12.1) when the absorbance at 300 nm was followed. A significantly different value (pK_a = 12.8) was found when the absorbance at 260 nm was used. This reflects the limitation of the use of spectrophotometric data. At both these wavelengths more than one species contributes to the measured absorbance. The difference in molar absorptivities of individual absorbing species is then reflected in the difference in the pH dependences of the absorbances at these two wavelengths. As the equilibria among I_a, I_b, and I_c in alkaline solutions could not be followed, relation of the measured pK_a value to values of pK^1_{OH}, pK^2_{OH}, and pK^3_{OH} remains uncertain. Attribution of the estimated pK_a of about 12.1 to the dissociation of the OH group in form I_c seems rather doubtful. Benzyl alcohol, which can be used as a model compound, has a pK_a = 15.6.[16] Neither the statistical factor nor the role of the ring strain can result in a shift of the pK_a values by more than 3 pK_a units. On the other hand, the value of pK_a = 12.1 is well within the range of pK_a values reported[12] for addition of OH^- ions to benzaldehydes bearing an electron-withdrawing group (such as the second formyl group). Furthermore, the presence and pH dependence of anodic waves of oxidation of OPA in alkaline solution—both on the DME (Figure 4) and on Au electrode—indicate the presence and role of the geminal diol anion (II_a). The shifts of the potentials of the anodic waves as a function of pH indicate in the presence of 1% acetonitrile for equilibria with constants K^1_{OH}

and K^2_{OH} an overall value of $pK_a^{exp} = 13.3$, where $pK_a^{exp} = K^1_{OH}K^2_{OH}/(K^1_{OH} + K^2_{OH})$.

The inflection point of the dissociation curve of the dependence of the polarographic anodic wave on pH in 1% acetonitrile ($pK' = 12.0$) is lower than $pK_a^{exp} = 13.5$, in agreement with the theory for formation of the geminal diol anion from aldehyde.[12] This reaction takes place in a reaction layer in the vicinity of the electrode surface. Calculation of the rate of addition of hydroxide ions to the carbonyl group is prevented by the above-mentioned difficulty in obtaining individual values of pK^1_{OH} and pK^2_{OH}.

The interpretation of the observed decreases of the cathodic reduction waves i_1 (with $pK' =$ ca. 12.0 in the presence of 1% acetonitrile and ca. 13.0 in 30% acetonitrile) (Figure 4) and i_2 ($pK' = 10.5$ in 1% acetonitrile and 10.8 in 30% acetonitrile) using DME may be complicated by the decrease in the rate of the surface protonation of the carbonyl group prior to the first electron uptake. A similar decrease of the currents with a pK' of about 12 was observed in solutions containing 1% acetonitrile, when the reduction took place on the glassy carbon electrode (Figure 5). These decreases may not have a simple relationship to processes involved in Scheme 3.

Conclusions

OPA exists in aqueous solutions in three forms that are in equilibrium: the hydrated form (I_a), the monohydrated acyclic form (I_b), and a cyclic hemiacetal form (I_c). It was generally assumed that OPA exists in such solutions practically entirely in the cyclic form I_c. Attempts[6] to obtain information about the position of the equilibria were restricted to the use of measurements of absorbances in the UV region. In the most frequently used wavelength ranges—at about 260 and 300 nm—more than one of the three forms I_a, I_b, and I_c absorbs. Molar absorptivities of individual forms at these wavelengths are not experimentally accessible. This prevents the determination of the concentration of individual forms at equilibrium. Under the assumption that the concentration of the acyclic hydrated form (I_b) is negligible and the absorbance at 300 nm is due solely to excitation of the π-electrons of the carbonyl groups of only I_a, an approximate equilibrium constant $K'_H = [I_c]/[I_a][H_2O]$ could be determined. With increasing temperature or increasing concentration of acetonitrile as a cosolvent, the equilibria are shifted in favor of the unhydrated form (I_a).

In NMR spectra, an addition of D_2O to a solution of OPA in CD_3CN results in formation of two new peaks. The attribution of these peaks to two isomeric forms[6] was proved to be incorrect. Experimental evidence strongly indicated that these two peaks—the surface areas of which differ—correspond to forms I_b and I_c. Due to the limited solubility of OPA in D_2O, NMR enabled investigation of the equilibria only in the presence of an excess of CD_3CN in a mixture with D_2O, where the equilibria are shifted in favor of forms I_b and I_a.

Information about the concentrations of all three forms of OPA present in aqueous solutions can be obtained by using electroanalytical techniques. Reduction currents obtained from $i-E$ curves recorded using the dropping mercury and glassy carbon electrodes enable determination of forms I_a and I_b. From the known analytical concentration of OPA, it is then possible to determine the concentration of the cyclic form I_c. This enabled obtaining values of equilibrium constants of the hydration—for the reaction between I_a and I_b (K_1)—and those of the cyclization—between I_b and I_c (K_2). As opposed to the situation involving use of absorbances, the data K_1 and K_2 based on measurements of polarographic limiting currents have well-defined physical meanings. Nevertheless, the need to obtain $[I_b]$ using the difference $i_2 - i_1$ and some degree of uncertainty regarding the number of electrons transferred in the course of reduction of individual species at the chosen pH limits the accuracy of the values of constants K_1 and K_2 reported here.

Combination of information based on electrochemical and spectrophotometric data indicated that in alkaline solutions of OPA a complex system of equilibria (Scheme 3) plays a role. The predominating feature is the important role of the oxidizable geminal diol anions (II_a), rather than that of anions of the cyclic hemiacetal (II_b).

Perhaps the most essential observation, made in this study, deals with the comparison of rates of hydration of OPA (obtained by spectrophotometry) with kinetics of dehydration of form I_c (gained from electrochemical data). The hydration of OPA, similarly to hydrations of other carbonyl compounds, is general-acid—base-catalyzed. The rate of dehydration, on the other hand, shows only specific-acid—base catalysis.

This observation rules out the possibility that the rates of both the hydration and dehydration are controlled by establishment of the same equilibrium as the rate-determining step. Both the hydration and dehydration of aliphatic and some heterocyclic aldehydes are general-acid—base-catalyzed. Hence, it seems plausible that the hydration of OPA is also controlled by the general-acid—base-catalyzed rate of the addition of water, followed by a fast ring closure. The rate of dehydration is then assumed to be controlled by the specifically catalyzed ring opening of the cyclic derivative I_c.

The pH dependences of the anodic currents of OPA were observed in alkaline solutions for oxidations at both mercury and gold electrodes. The shapes of these dependences resemble those obtained for other benzaldehydes.[12] This indicates that the species oxidized in solutions of OPA is also a geminal diol anion. For other benzaldehydes, which are practically not hydrated, the geminal diol anion results from an addition of hydroxide ions to the formyl group. The geminal diol anion derived from OPA can be formed both by an addition of hydroxide ions to form I_a and by dissociation of an OH group in form I_b. This complication and a possible role of dissociation of an OH group of form I_c prevents currently a quantitative evaluation of the rate of formation of the geminal diol anion.

The oxidation of OPA was observed to take place when mercury and gold electrodes were used, but not on the glassy carbon electrode. In the potential range where the oxidation in alkaline solutions was observed, the mercury and gold are covered by a layer of an adsorbed slightly soluble hydroxo complex of the metal. The oxidation of the geminal diol anion (II_a) hence takes place by an electron transfer on the surface of the adsorbed layer, as was proposed earlier for oxidation of a pyridinecarboxaldehyde by Volke.[17] The geminal diol anion (II_a) is thus formed from forms I_a and I_b in a layer of solution in the vicinity of the surface of the adsorbed layer. The anodic current is controlled by the rate of formation of II_a in this reaction layer.

Analytical methods for the determination of amino acids, based on reaction of OPA in the presence of a nucleophile that is not able to form a cyclic derivative and on a following reaction of the product of nucleophilic addition with amino acids, have been carried out in the range between pH 8 and pH 11. This investigation offers information on which forms of OPA can be present in this pH range. It also indicates which chemical reactions control formation of the species of OPA that are available for reactions with added nucleophile and amino acids.

Acknowledgment. Some initial experiments, involving some reactions of OPA, have been carried out by K. Vercoe and M. S. Byamak.

Supporting Information Available: More detailed information about the polarographic data, additional tables of rate constants and of temperature and current dependence on concentration and on pH, graphs of limiting current vs $h^{1/2}$, peak current vs $[H_2O]$ and $\upsilon^{1/2}$, potential vs pH, peak current vs [OPA], UV spectra, absorbance vs time, and k_{obs} vs pH, $[H^+]$, and $[OH^-]$, and derivation of constants K_1, K_2, and K_H. These materials are available free of charge via the Internet at http://pubs.acs.org.

References and Notes

(1) (a) Roth, M. *Anal. Chem.* **1971**, *43*, 880. (b) Molnár-Perl, I. *J. Chromatogr., A* **2001**, *913*, 283. (c) Molnár-Perl, I.; Vasanits, A. *J. Chromatogr., A* **1999**, *835*, 73. (d) Molnár-Perl, I.; Bozor, I. *J. Chromatogr., A* **1998**, *798*, 37. (e) Simons, S. S.; Johnson, D. F. *Anal. Biochem.* **1978**, *90*, 705. (f) Stobaugh, J. F.; Repta, A. J.; Sternson, L. A.; Garren, K. W. *Anal. Biochem.* **1983**, *135*, 495. (g) Jacobs, W. A.; Leburg, M. W.; Madaj, E. J. *Anal. Biochem.* **1986**, *156*, 334. (h) Zuman, P. *Chem. Rev.* **2003**, *104* (7), 3217.

(2) (a)Simons, S. S., Jr.; Johnson, D. F. *J. Am. Chem. Soc.* **1976**, *98*, 7098. (b) Simons, S. S., Jr.; Johnson, D. F. *Anal. Biochem.* **1977**, *82*, 250. (c) Metz, P. A.; Gehas, J.; Spriggle, J.; Veenig, H. *J. Chromatogr.* **1985**, *330*, 307. (d) Tippet, P. A.; Clayton, B. E.; Mallet, A. I. *Biomed. Environ. Mass Spectrosc.* **1987**, *14*, 737. (e) de Montigny, P.; Stobaugh, J. F.; Givens, R. S.; Carlson, R. G.; Srinivasachar, K.; Sternson, L. A.; Higuchi, T. *Anal. Chem.* **1987**, *59*, 1096. (f) Sternson, L. A.; Stobaugh, J. F.; Repta, A. J. *Anal. Biochem.* **1985**, *144*, 233.

(3) (a) Trepman, E.; Chen, R. F. *Arch. Biochem. Biophys.* **1980**, *204*, 524. (b) Wong, O. S.; Sternson, L. A.; Schowen, R. L. *J. Am. Chem. Soc.* **1985**, *107*, 6421.

(4) (a) Simons, S. S., Jr.; Johnson, D. F. *J. Org. Chem.* **1978**, *43*, 2886. (b) Gladilovich, D. B.; Kartsova, L. A.; Zakharova, I. O. *Russ. J. Gen. Chem.* **1993**, *63*, 1474.

(5) Salem, N.; Zuman, P. *Anal. Chem.* **2006**, *78* (22), 7802.

(6) (a) McDonald, R. S.; Martin, E. V. *Can. J. Chem.* **1974**, *57*, 506. (b) Bowden, L.; El-Kaissi, F. A.; Nadvi, N. S. *J. Chem. Soc., Perkin Trans. 2* **1979**, 642.

(7) Seekles, L. *Recl. Trav. Chim. Phys-Bas* **1923**, *42*, 706.

(8) (a) Furman, N. H.; Norton, D. R. *Anal. Chem.* **1954**, *26*, 1111. (b) Norton, D. R.; Furman, N. H. *Anal. Chem.* **1954**, *26*, 1116. (c) Person, M.; Meunier, J. M.; Beau, D. *Compt. Rend.* **1972**, *275c*, 527.

(9) Heyrovsky, J.; Kalousek, M. *Collect. Czech. Chem. Commun.* **1939**, *11*, 464.

(10) Bover, W. J.; Johnson, D.; Bymak, M. S.; Zuman, P. *Indian J. Chem.* **2003**, *42A*, 744.

(11) BaymaK, M. S.; Vercoe, K. L.; Zuman, P. *J. Phys. Chem. B* **2006**, *109*, 21928.

(12) Bover, W. J.; Zuman, P. *J. Electrochem. Soc.* **1975**, *122*, 368.

(13) Assiongbon, K. A.; Roy, D. *Surf. Sci.* **2005**, *594*, 99.

(14) Heyrovsky, J.; Kuta, J. *Principles of Polarography*; Academic Press: New York, 1965; pp 172−175.

(15) Szyper, M.; Zuman, P. *Anal. Chim. Acta* **1976**, *21*, 687.

(16) Murto, J. *Acta Chem. Scand.* **1964**, *18*, 1043.

(17) Volke, J. J. *Electroanal. Chem.* **1965**, *10*, 344.